Indirect Current Control for Seamless Transfer of Three-Phase Utility Interactive Inverters

Junbum Kwon, Sunjae Yoon, and Sewan Choi, *Senior Member, IEEE*

***Abstract*—This paper proposes an indirect current control algorithm for seamless transfer of three-phase utility-interactive voltage source inverters. With the proposed method the inverter is able to provide critical loads with a stable and seamless voltage during the whole transition period including both clearing time and control mode change. The LCL filter design which is suitable for the indirect current control is also proposed to meet the harmonic limits. The proposed control method is validated through simulation and experiment.**

***Index Terms*—Indirect current control, LCL filter, seamless transfer, three-phase inverter, utility-interactive inverter.**

I. Introduction

RECENTLY, new and renewable energy sources such as fuel cells, photovoltaic and wind turbines have been recognized as major alternatives to fossil fuels. Alternative energy sources which range from 1 kW to several hundred MW levels generate either dc or variable frequency ac and are normally connected to the grid as a distributed generation (DG) system. Utility-interactive inverters have been playing an important role in DG. The utility-interactive inverter should operate in both grid-connected and stand-alone modes to provide uninterrupted and continuous power to critical loads, for example, such as power supplies for mechanical balance of plant (MBOP) in fuel cell systems. During the grid-connected mode the inverter is operated to inject power from the DG unit to the grid. When a fault occurs in the grid, a recloser switch is open and the DG unit enters into islanding. Then, the inverter should detect the islanding and cease to energize the grid by disconnecting the DG unit from the grid within two seconds which is a required clearing time [1].

Fig. 1 shows a detailed transfer sequence from the grid-connected mode to the stand-alone mode. The clearing time consists of detection time, adjustable time delay and operating time of an inverter switch. The detection time is defined as the minimum length of time from turn-off of the recloser, which is considered as the islanding, to change in state of the inverter's output dedicated to controlling the inverter switch that is usually a circuit breaker. This is often on the order of 8 to 16 ms. The adjustable time delay is the intentional time added to the detection time in order to provide the desired clearing time. This may be adjustable from zero to several seconds. The operating time of the circuit breaker should be considered in this mode transfer sequence and is often longer than 50 ms. During this unintentional islanding, voltage across the critical load may experience severe transient state since the inverter switch is still closed and the voltage is determined by the amount of the injected power and unknown load condition. Further, there exists a large transient across the critical load even after actual turn-off of the inverter switch since the conventional controller should be changed from the current controlled mode to the voltage controlled mode.

A simulation result of the conventional control method is shown in Fig. 2 to illustrate the transient associated with the mode transfer that observes the sequence shown in Fig. 1. Excessive transient voltage across the critical load can be seen during the clearing time as well as the control mode change which is performed right after the actual turn off of the switch. Thus, one of the key functions of the utility-interactive inverter is seamless transfer between grid-connected and stand-alone modes, which is a main focus of this research.

A sequence for smooth mode transfer between two modes has been addressed and implemented in [2], [3]. A control technique proposed in [4] reduces turn-off time of a static switch (SCR) by controlling voltage across the grid-side inductor, which results in quick grid current decrease. The voltage transient across the critical load could last longer if circuit breakers are used as an inverter switch since operating time is at least several tens of millisecond. In order to alleviate the transient voltage and inrush current associated with operating time of a circuit breaker a control algorithm using the feedback status of circuit breakers has been proposed [5]. However, the control methods for mode transfer proposed in [2]–[5] have a drawback. For mode transfer the inverter should change its controller from current control to voltage control, which can cause large voltage or current spikes. A control method for the single-phase system has been proposed to eliminate the transient associated with the control mode change by utilizing both current and voltage controllers in both grid-tied and off-grid modes [6]. However, this method cannot avoid the voltage transient across the critical load during the clearing time. Further, none of the aforementioned control algorithms for seamless transfer [2]–[6] considered the transient state during the whole transition period including both clearing time and control mode change.

Manuscript received December 26, 2010; revised March 15, 2011 and May 12, 2011; accepted June 23, 2011. Date of current version January 9, 2012. This work was supported by the New and Renewable Energy Program of the Korea Institute of Energy Technology Evaluation and Planning, Grant 2008-N-FC12-J-04-2100, funded by the Korea government Ministry of Knowledge Economy. Recommended for publication by Associate Editor Q.-C. Zhong.

J. Kwon and S. Yoon are with the LS Industrial Systems, Anyang 431-080, Korea (e-mail: jbkwona@lsis.biz; sjyoona@lsis.biz).

S. Choi is with the Seoul National University of Science and Technology (Seoul Tech), Department of Control and Instrumentation Engineering, 172 Kongneung-Dong, Nowon-Gu, Seoul 139-743, Korea (e-mail: schoi@seoultech.ac.kr).

Color versions of one or more of the figures in this paper are available online at http://ieeexplore.ieee.org.

Digital Object Identifier 10.1109/TPEL.2011.2161335

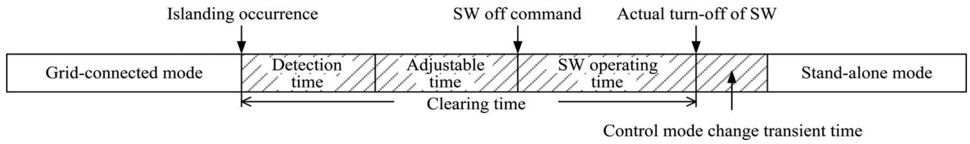

Fig. 1. Transfer sequence from grid-connected to stand-alone mode [1].

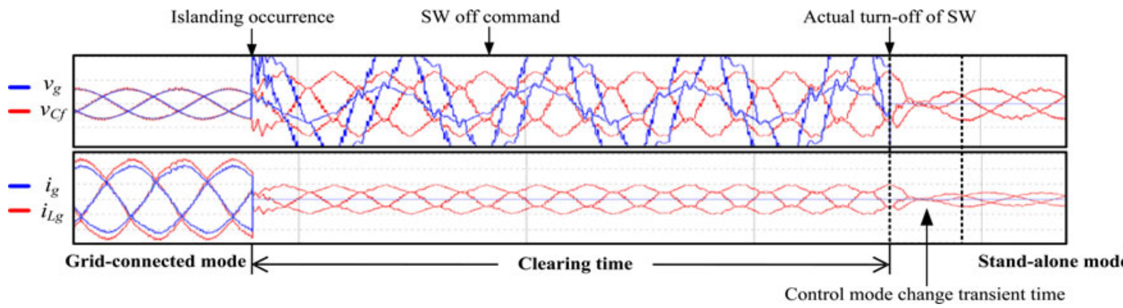

Fig. 2. Simulation of mode transfer with the conventional control.

An indirect current control method was proposed for seamless transfer of a single-phase utility interactive inverter, where the transient associated with control mode change has significantly been reduced by controlling the peak value of the output current with an inner voltage loop in both grid-connected and stand-alone modes [7]. A drawback of this method is that the inverter is not able to control instantaneous values in the grid-connected mode since peak value of inductor current is used for current control, which may result in inaccurate instantaneous values or dc offset of grid current during the transient state. Further, the desired resonant frequency and filter cut-off frequency which vary according to variation of grid-side inductance may not be obtained since the LCL filter design was not based on the exact LCL model. Also, the grid current may not meet the harmonic limits since the ripple rate of the grid current was not considered in the grid-side inductance calculation.

This paper proposes a control algorithm for seamless transfer of three-phase utility-interactive inverters. By controlling the capacitor voltage in both grid-connected and stand-alone modes the proposed method is capable of providing critical loads with a stable and seamless voltage during the whole transition period including both clearing time and control-mode-change transition. Also, the proposed method is able to guarantee accurate instantaneous values of injected current without dc offset during the transient state by introducing dq-transformation to control instantaneous values of the output current. Further, an LCL filter design method which is suitable for indirect current control is proposed to achieve the desired resonant frequency and filter cut-off frequency and meet the harmonic limits by considering the ripple rate of the grid current in the grid-side inductance calculation.

II. Proposed Control Algorithm

A. Operating Principle of Three-phase Indirect Current Control

Fig. 3 shows the circuit diagram of a three-phase utility-interactive inverter for the DG system. The three-phase inverter

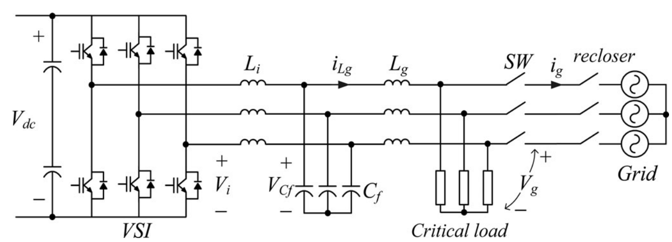

Fig. 3. Circuit diagram of a three-phase utility-interactive inverter with a critical load.

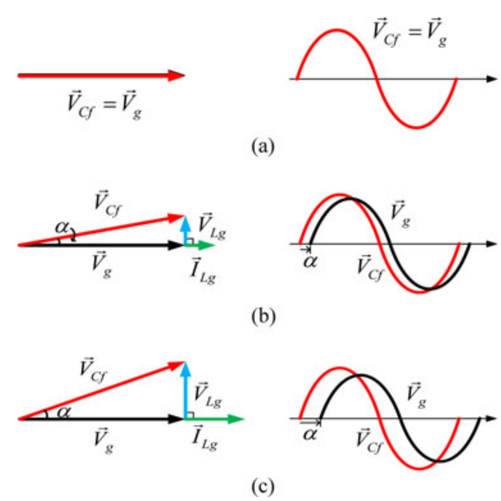

Fig. 4. Phasor diagram illustrating the operating principle of the proposed indirect current control during the grid-connected mode (a) no current injection, (b) medium current injection, and (c) rated current injection.

with LCL filters is connected to the grid through an inverter switch, a step-up transformer, and a recloser. A critical load is located between the LCL filter and the switch. Fig. 4 shows a phasor diagram illustrating the operating principle of the proposed indirect control for the three-phase utility interactive inverter. The basic idea of the proposed control is to regulate the grid-side inductor current I_{Lg} by controlling the magnitude and

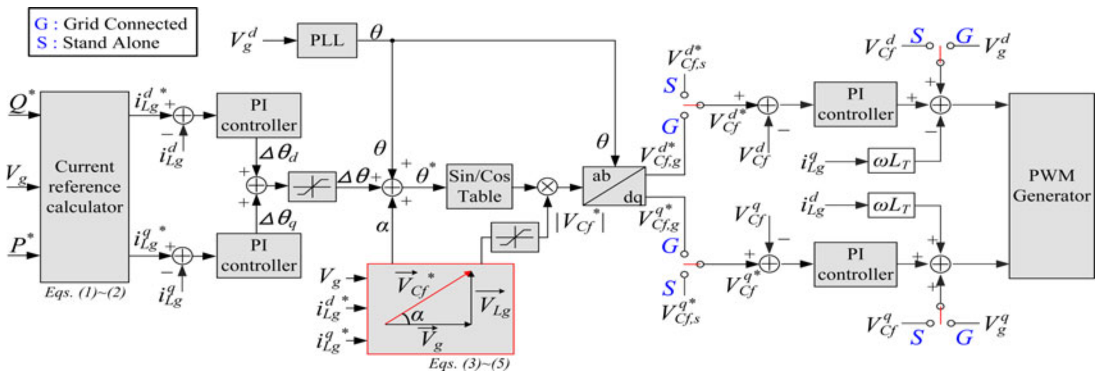

Fig. 5. Block diagram of the proposed indirect control for a three-phase utility-interactive inverter.

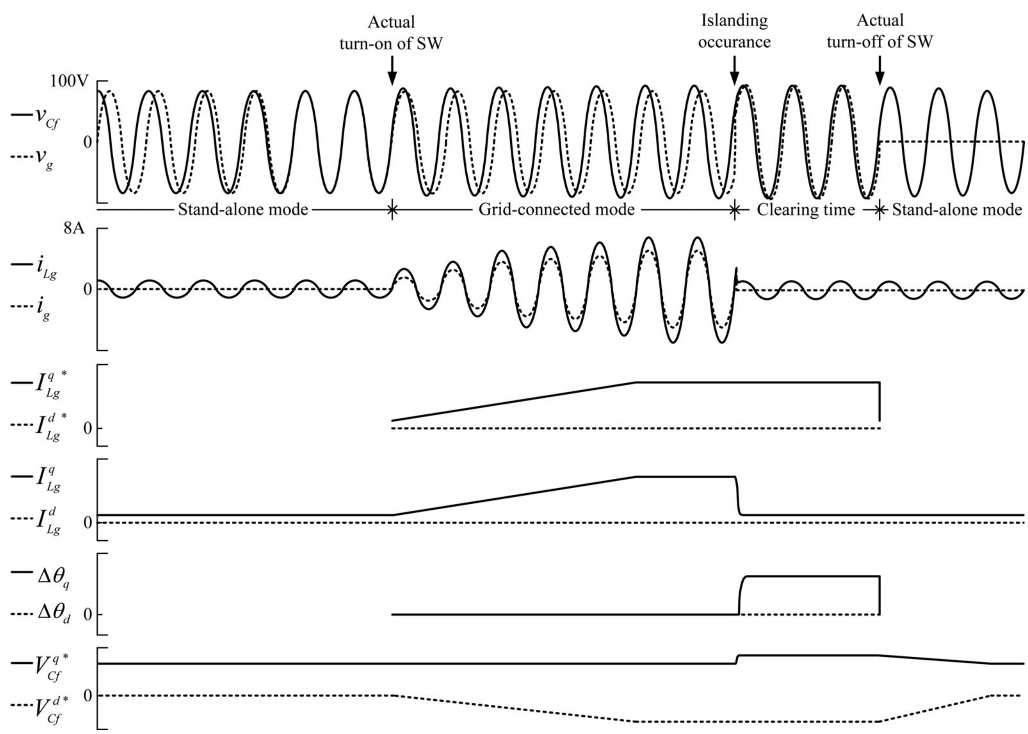

Fig. 6. Key waveforms of the proposed indirect control for seamless mode transfer of a three-phase utility-interactive inverter.

phase angle of capacitor voltage V_{Cf} so that the desired magnitude of current which is in phase with the utility voltage is injected to the grid. In Fig. 4(a) capacitor voltage V_{Cf} is being controlled to be equal in the magnitude and phase to the grid voltage so that no phase of V_{Cf} such that voltage V_{Lg} is perpendicular to grid voltage V_g, the amount of injected current I_{Lg} that is in phase with V_g can be increased, as shown in Fig. 4(b) and (c).

The dq-current commands on the grid-side inductor can be calculated as follows if the desired real and reactive power are assumed to be P^* and Q^*, respectively

$$I_{Lg}^{q*} = \frac{(2/3)\left(P^* V_g^q + Q^* V_g^d\right)}{\left(V_g^d\right)^2 + \left(V_g^q\right)^2} \tag{1}$$

$$I_{Lg}^{d*} = \frac{(2/3)\left(P^* V_g^d - Q^* V_g^q\right)}{\left(V_g^d\right)^2 + \left(V_g^q\right)^2}. \tag{2}$$

Then, the voltage across grid-side inductor should be

$$V_{Lg}^d = \omega L_g \times I_{Lg}^{q*}. \tag{3}$$

Therefore, the required magnitude and angle of capacitor voltage V_{Cf} to generate P^* and Q^* can be obtained by

$$|V_{Cf}|^* = \sqrt{\left(V_g^q\right)^2 + \left(V_{Lg}^d\right)^2} \tag{4}$$

$$\alpha = \tan^{-1}\left(\frac{V_{Lg}^d}{V_g^q}\right). \tag{5}$$

Fig. 5 shows the proposed control block diagram for grid-connected and stand-alone operations of the three-phase utility-interactive inverter. The controller consists of an outer current control loop for regulating the desired amount of injection current and an inner voltage control loop for controlling instantaneous capacitor voltage. Both outer current and inner voltage

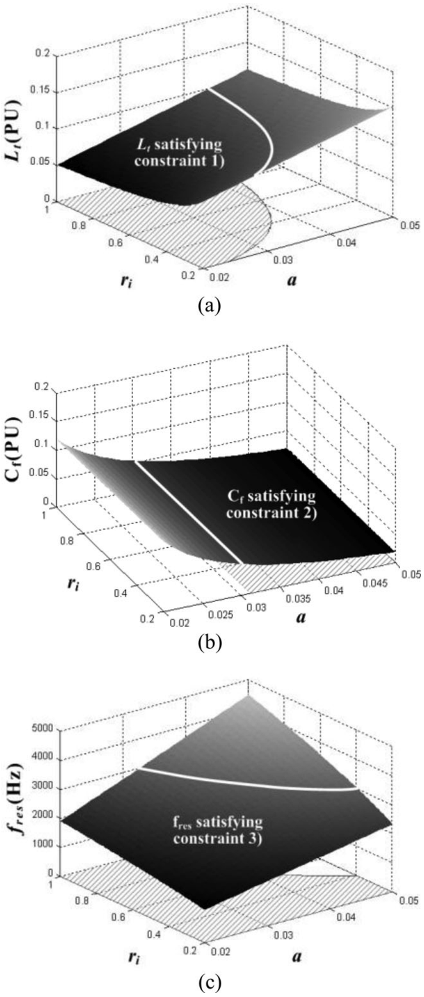

Fig. 7. (a) Total inductance. (b) Capacitance. (c) Resonant frequency as a function of a and r_i when $f_s = 10\,\text{kHz}$ and $r_g = 0.003$.

loops are used for the grid-connected mode. The dq-current commands I_{Lg}^{d*} and I_{Lg}^{q*}, which are obtained by (1) and (2), respectively, are fed to PI controllers [15]. Outputs of the PI controllers $\Delta\theta_d$ and $\Delta\theta_q$, which denote signals for the compensating phase and magnitude errors of current reference, are summed together and added to angle α and reference angle of the grid θ to generate a reference angle θ^* of the capacitor voltage. The values from the sine and cosine table are multiplied by the reference magnitude $|V_{Cf}^*|$ of the capacitor voltage to generate capacitor voltage commands $V_{Cf,g}^{d*}$ and $V_{Cf,g}^{q*}$ in the synchronous reference frame. In order to simplify implementation, the LCL filter is approximated to a simple $L_T(L_g+L_i)$ filter, and the decoupling effect due to C_f could be disregarded [14].

The error between the commanded and measured values is fed to a voltage compensator to generate PWM signals for the inverter. Only the inner voltage loop is used for the stand-alone mode. The PI controllers are used to regulate the capacitor voltage commands $V_{Cf,s}^{d*}$ and $V_{Cf,s}^{q*}$ which become 0 and rated peak value of line-to-neutral grid voltage, respectively.

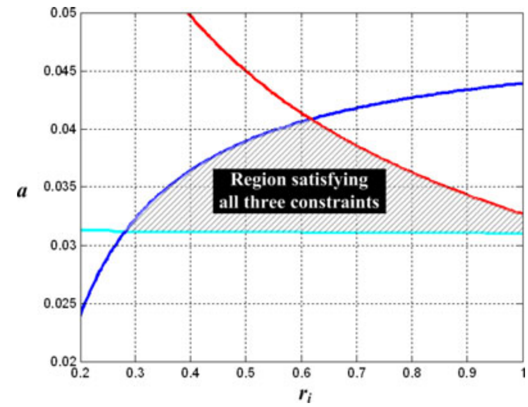

Fig. 8. Region that satisfies all three constraints in Fig. 7.

TABLE I
SIMULATION AND EXPERIMENTAL SPECIFICATION

Rated power	1kW
Rated power(stand-alone mode)	1.2kW
Critical load power	1.2kW
Grid voltage(*line-to-line*)	110V/60Hz
DC-link voltage	250V
Switching frequency	10kHz
L_i	3000μH
C_f	2μF
L_g	5000μH

B. Mode Transfer Sequence

The proposed procedure to change from grid-connected to the stand-alone mode is summarized as follows.

1) Detect a fault on the grid.
2) Give a turn-off signal to the inverter switch.
3) Wait until the status of the inverter switch is in the off-state.
4) Switch the operation mode from the grid-connected mode "*G*" to the stand-alone mode "*S*."
5) Gradually change voltage references $V_{Cf,s}^{d*}$ and $V_{Cf,s}^{q*}$ from the last values of $V_{Cf,s}^{d*}$ and $V_{Cf,s}^{q*}$ to the desired 0 and rated peak value of line-to-neutral grid voltage, respectively.

Fig. 6 shows key waveforms of the proposed indirect control for seamless transfer between the grid-connected and stand-alone mode. When the grid fault occurs, a recloser is open and the grid current is dumped into the critical load in the conventional control, which could cause a transient voltage across the load. However, in the proposed control magnitude reference of capacitor voltage V_{Cf}^* and compensation terms for phase reference which are outputs from the current controllers are restricted to appropriate values by limiters, leading to negligible transient voltage across the critical load. The voltage across the critical load is well regulated and maintained as sinusoidal waveform throughout the clearing time. It is seen that the transient voltage across the load does not occur even at actual turn-off of the inverter switch since the voltage control is maintained throughout the whole operation period. In the meanwhile, the proposed procedure to change from stand-alone to grid-connected mode is summarized as follows.

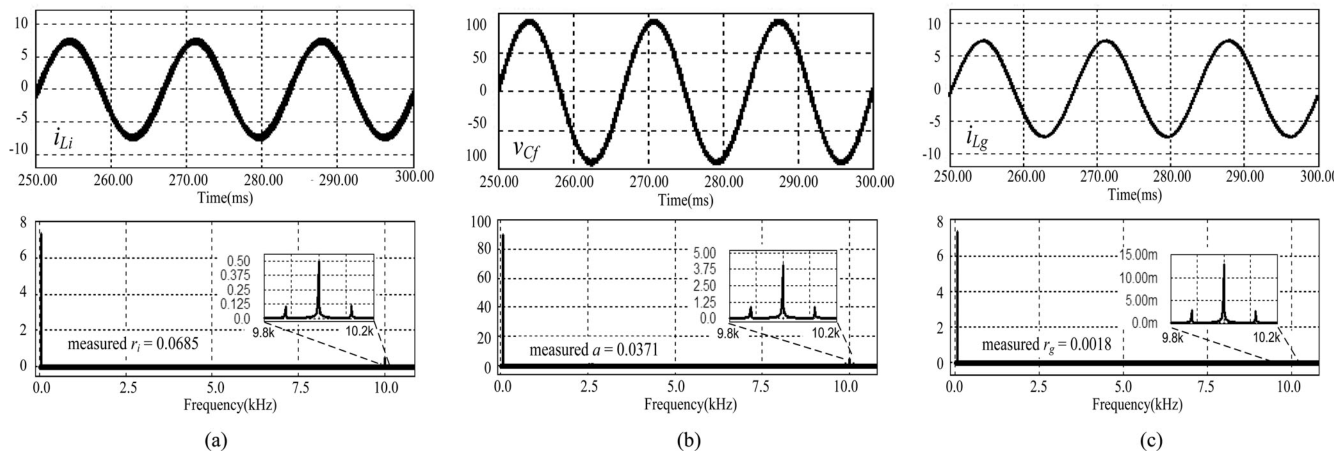

Fig. 9. Simulation results showing the validity of the proposed LCL filter design method. (a) Waveforms and FFT of inverter-side inductor currents. (b) Waveforms and FFT of capacitor voltages. (c) Waveforms and FFT of grid-side inductor currents.

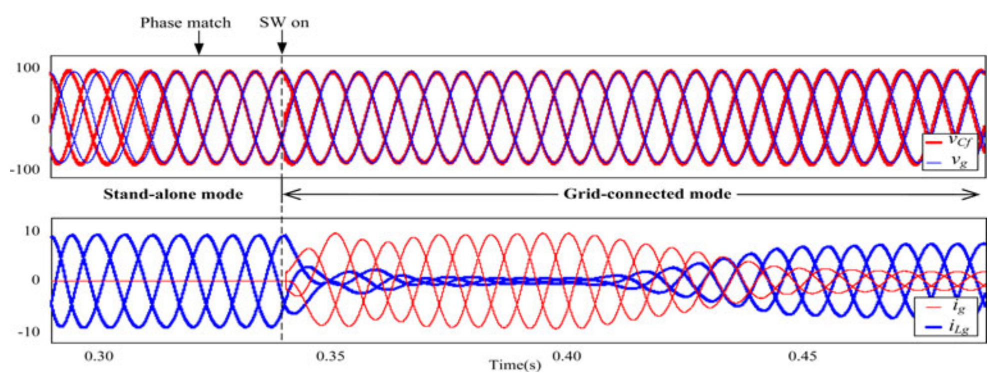

Fig. 10. Simulation results of the proposed control showing a mode transfer from stand-alone mode to grid-connected mode (the inverter is being operated in the grid supporting mode as shown in Fig. 12).

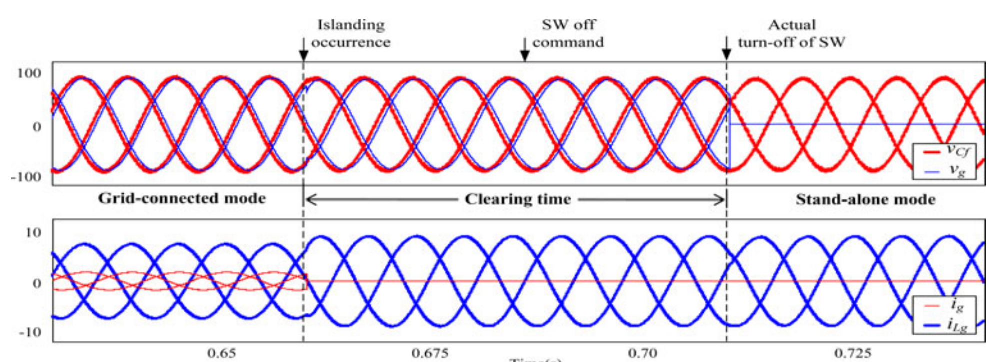

Fig. 11. Simulation results of the proposed control showing a mode transfer from a grid-connected mode to a stand-alone mode.

1) Detect that the grid voltage is within the normal operating voltage range.
2) Adjust the phase and magnitude of the inverter output voltage to match the grid voltage.
3) If the inverter output voltage matches the grid voltage, turn on the inverter switch.
4) Wait until the status of the inverter switch becomes on-state.
5) Switch the operation mode from stand-alone mode "S" to grid-connected mode "G.".
6) Gradually increase the current reference to the desired value.

III. LCL Filter Design for Proposed Control Technique

For the grid interface, the harmonics of injected current should be limited according to the harmonic limits presented in the standards, e.g., IEEE 1547-2003. LCL filters are usually designed in such a way that inverter-side inductor is firstly chosen to attenuate its ripple current and then a capacitor and grid-side inductor is added to meet the harmonic limits [8], [9]. In the proposed indirect current control, the LCL filter is designed in such a way that the LC-filter is firstly chosen to have desired capacitor voltage ripple attenuation at the switching frequency, and then grid-side inductor is added to satisfy the harmonic requirement. The proposed LCL filter design procedure is detailed in the following.

Given rated inverter output power P, grid voltage V_g, dc-link voltage V_{dc}, switching frequency $f_{\mathrm{sw}} = \omega_{\mathrm{sw}}/2\pi$ and desired ripple rate of the grid-side inductor current $r_g = I_{Lg,\mathrm{sw}}/I_{Lg,1}$, the inverter output power can be expressed as, assuming $I_{Li,1} \gg I_{Cf,1}$

$$P = 3V_g \times I_{Lg,1} \approx 3V_g \times I_{Li,1}. \tag{6}$$

SPWM assumed with the modulation index of 0.8 is used as an inverter switching method and the switching frequency is much higher than the fundamental frequency; hence, the rms value of the inverter output voltage at the switching frequency $V_{i,\mathrm{sw}}$ becomes [10]

$$V_{i,\mathrm{sw}} = 0.818 \times 0.5V_{\mathrm{dc}}/\sqrt{2}. \tag{7}$$

Also, the rms value of the grid-side inductor current at the switching frequency can be obtained by

$$I_{Lg,\mathrm{sw}} = \frac{V_{Lg,\mathrm{sw}}}{\omega_{\mathrm{sw}} L_g} = \frac{V_{Cf,\mathrm{sw}}}{\omega_{\mathrm{sw}} L_g} \tag{8}$$

where $V_{Lg,\mathrm{sw}} = V_{Cf,\mathrm{sw}} - V_{g,\mathrm{sw}} = V_{Cf,\mathrm{sw}}$, if the grid voltage is assumed to be pure sinusoidal. Then, from (6)–(8), the grid-side inductor can be obtain by

$$L_g = \frac{0.867 \cdot a \cdot V_{\mathrm{dc}} \cdot V_g}{\omega_{\mathrm{sw}} \cdot r_g \cdot P} \tag{9}$$

where $a = V_{Cf,\mathrm{sw}}/V_{i,\mathrm{sw}}$ is capacitor voltage ripple attenuation at the switching frequency. Assuming $V_{i,\mathrm{sw}} \gg V_{Cf,\mathrm{sw}}$, the rms value of the inverter-side inductor current at the switching frequency can be obtained by

$$I_{Li,\mathrm{sw}} = \frac{V_{Li,\mathrm{sw}}}{\omega_{\mathrm{sw}} L_i} = \frac{V_{i,\mathrm{sw}}}{\omega_{\mathrm{sw}} L_i}. \tag{10}$$

Then, from (6), (7), and (10) the inverter-side inductor is determined by

$$L_i = \frac{0.867 \cdot V_{\mathrm{dc}} \cdot V_g}{\omega_{\mathrm{sw}} \cdot r_i \cdot P} \tag{11}$$

where $r_i = I_{Li,\mathrm{sw}}/I_{Li,1}$ $(1>r_i>r_g)$ is the ripple rate of the inverter-side inductor current which is usually selected to be between 0.1 and 0.5. From the LCL model [11], the rms value of the capacitor voltage at the switching frequency can be obtained by

$$V_{Cf,\mathrm{sw}} = \frac{L_g}{\omega_{\mathrm{sw}}^2 L_g C_f L_i + (L_g + L_i)} V_{i,\mathrm{sw}}. \tag{12}$$

Then, the capacitor is determined by

$$C_f = \frac{1}{\omega_{\mathrm{sw}}^2 a}\left(\frac{1-a}{L_i} + \frac{\omega_{\mathrm{sw}} \cdot r_g \cdot P}{0.867 \cdot V_{\mathrm{dc}} \cdot V_g}\right). \tag{13}$$

From (6), (7), (9), and (11) the total inductance in PU is obtained by

$$L_{T\_pu} = L_{i\_pu} + L_{g\_pu} = \frac{1.022\omega_b}{\omega_{\mathrm{sw}} r_i} + \frac{1.022 \cdot a \cdot \omega_b}{\omega_{\mathrm{sw}} r_g}. \tag{14}$$

Also, from (6), (7), and (13) the filter capacitance in PU is obtained by

$$C_{f\_pu} = \frac{1}{\omega_{\mathrm{sw}}^2 a}\left(\frac{1-a}{L_{i\_pu}} + 9.787 \cdot \frac{\omega_b \cdot \omega_{\mathrm{sw}} \cdot r_g}{a}\right). \tag{15}$$

Then from (14) and (15) the resonant frequency can be obtained by

$$f_{\mathrm{res}} = \frac{1}{2\pi}\sqrt{\frac{\omega_{\mathrm{sw}}^2 a\,(ar_i + r_g)}{(ar_i + 10\omega_b^2 r_g - a^2 r_i)}}. \tag{16}$$

Fig. 7(a), (b), and (c) show the total inductance, capacitance, and resonant frequency, respectively, as a function of ripple attenuation at the switching frequency "a" and ripple rate of the inverter-side inductor current "r_i." In the meanwhile, three constraints according to filter design guideline presented in [8] are as follows: 1) Total inductance should be less than 0.1 PU to limit the ac voltage drop across the inductors. 2) The filter capacitance should be limited by the decrease of the power factor at rated power (generally less than 0.05PU). 3) The resonant frequency should be in a range between the system bandwidth and one-half of the switching frequency. Each dashed area of Fig. 7 is the region that satisfies respective constraint described earlier. A region that satisfies all three constraints in Fig. 7 is shown in Fig. 8, and any desired values within the region can be chosen. Then, final filter values of L_i, C_f, and L_g can be calculated using (9), (11), and (13).

IV. Simulation Results

To confirm the validity of the proposed indirect current control algorithm and filter design method, a simulation has been performed using PSIM. The system parameters for simulation studies are given in Table I. For consistency between the simulation and experiment the inverter is assumed to be operated in the grid-supporting mode.

Assuming the desired ripple rate of the grid-side inductor $r_g = 0.003$, the LCL filter values are calculated according to the design method mentioned in Section III, and the resultant values are shown in Table I. Also, the simulated waveforms and FFT are shown in Fig. 9 As shown in Fig. 9(a) and (b), the measured ripple rate of inverter-side inductor current r_i and capacitor voltage ripple attenuation a are 0.0685 and 0.0371, respectively, which are close to calculated values of $r_i = 0.07$ and $a = 0.042$. Fig. 9(c) shows that the measured ripple rate of grid-side inductor current is 0.0018 which is within the specified limit of 0.003. The measured THD of the grid current is 0.23%.

Fig. 10 shows the simulation result of the transfer from the stand-alone mode to the grid-connected mode. It can be seen that the inverter is operated to the match phase and magnitude of the inverter output voltage to the grid voltage. After the phased match the inverter switch is closed, the grid current supplies the critical load and at the same time the grid-side inductor current

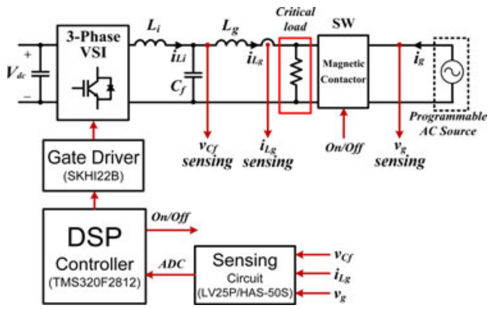

Fig. 12. Block diagram of the experimental setup.

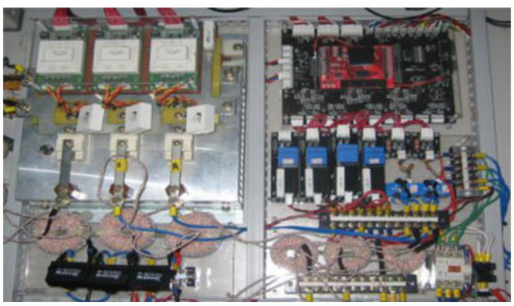

Fig. 13. Photograph of the laboratory prototype.

reduces to zero since the commanded real and reactive power are zero in the beginning. And then grid current i_{Lg} is increased according to its commanded real power while i_g is decreased since the inverter is in the supporting mode.

Fig. 11 shows the simulation result of the transfer from grid-connected mode to the stand-alone mode. The inverter is injecting a current into the grid. At the moment of islanding occurrence, there exists a little transient voltage across the critical load, which is generated by the turn-off of recloser switch. During the clearing time, the capacitor and load voltages do not go through any transient. After the clearing time the inverter switch is turned off, and the controller is changed from grid-connected mode to the stand-alone mode. It should be noted that there is no transient state across the load according to the control mode change since the controller maintains voltage control.

V. Experimental Results

A 1 kW utility interactive inverter has been built to verify the proposed control method with the parameters shown in Table I. Fig. 12 shows the experimental setup for the proposed utility-interactive inverter system. A programmable ac source is used to emulate the utility grid, and therefore the inverter should be operated in grid supporting mode. A magnetic contactor which is used as an inverter switch is located between critical load and the programmable ac source. The TMS320F2812 chip is used to implement the proposed control and the capacitor voltage, grid-side inductor current and grid voltage are sampled. An on/off signal for magnetic contactor is generated by the DSP controller.

Fig. 13 shows the photograph of the laboratory prototype. Fig. 14 shows the experimental result of the transfer from the stand-alone mode to the grid-connected mode. It can be seen

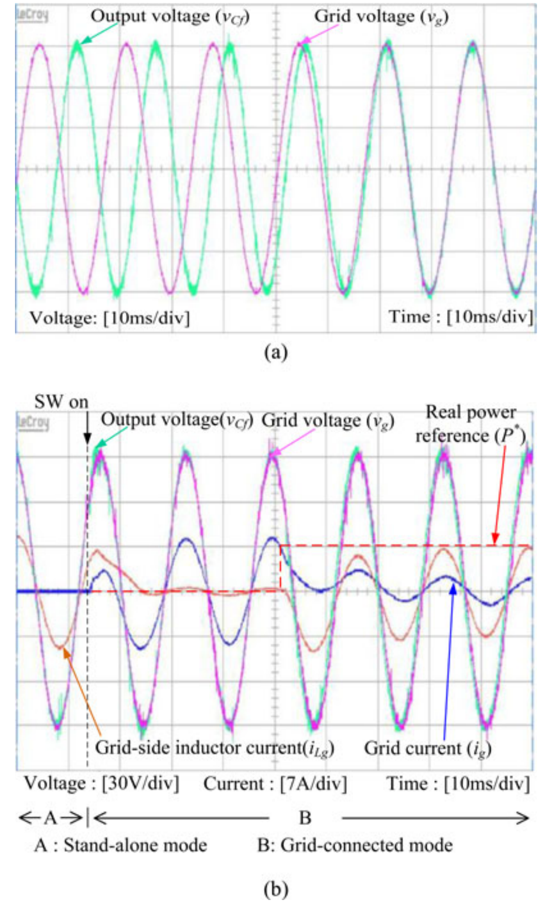

Fig. 14. Experimental waveforms of the proposed control showing a mode transfer from a stand-alone mode to a grid-connected mode. (a) Phased match. (b) Turn-on of inverter switch and current injection.

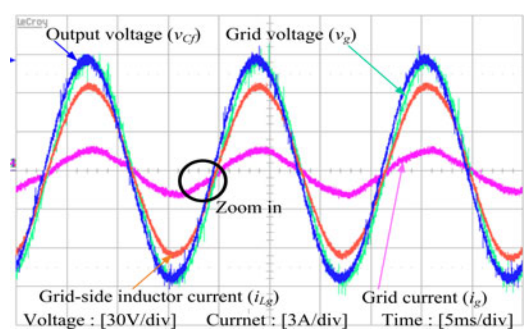

Fig. 15. Experimental waveforms of the proposed control method with current command on the grid-side inductor of 3.2 A.

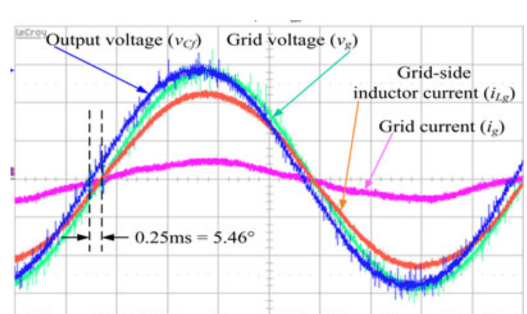

Fig. 16. Extended waveforms of Fig. 15.

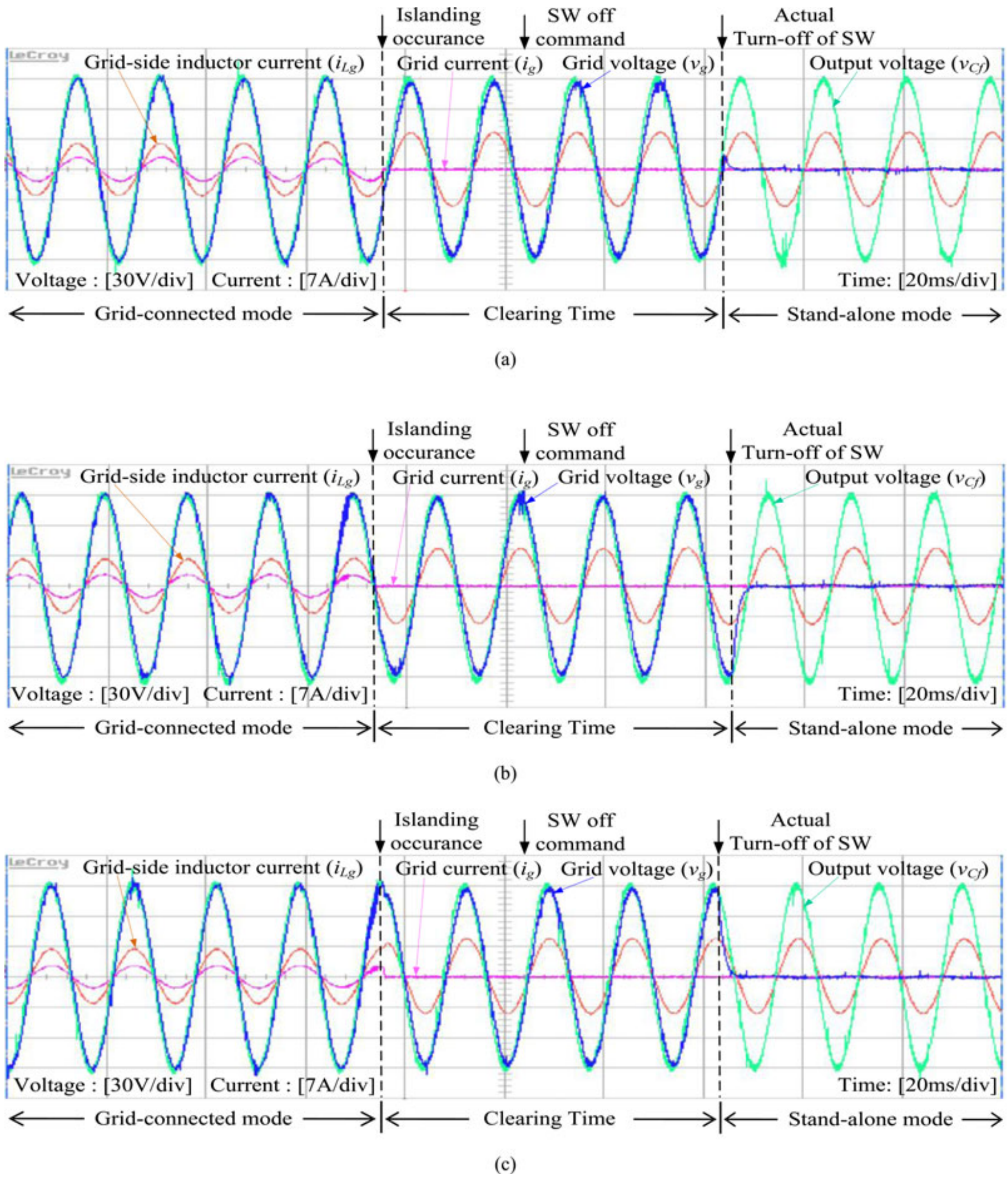

Fig. 17. Experimental waveforms of the proposed control method showing the mode transfer from grid-connected mode to a stand-alone mode phase (a), phase (b), and phase (c).

from Fig. 14(a) that the inverter is operated to the match phase and the magnitude of the inverter output voltage to the grid voltage. After the phased match the inverter switch is closed, the grid current supplies the critical load and at the same time the grid-side inductor current reduces to zero since the commanded real and reactive power are zero in the beginning. And then grid current i_{Lg} is increased according to its commanded real power, as shown in Fig. 14(b). Fig. 15 shows the experimental waveforms of the proposed control during the grid-connected mode. The current command on the grid-side inductor is 3.2 A, and theoretical magnitude and phase angle of capacitor voltage $|V_{Cf}|$ and α are calculated to be 90.22 V and 5.42°, respectively. It can be seen from Fig. 16 that the measured magnitude and phase angle of capacitor voltage are about 90.3 V and 5.46°, respectively. The measured THD of the grid current is 0.86% at 1 kW. Fig. 17 shows the experimental waveforms of the transfer from grid-connected mode to stand-alone mode. The transient voltage across the load at the moment of islanding occurrence is negligible. Any noticeable transient is not observed across the load throughout the whole transition period including the clearing time and control mode change which is performed right after actual turn-off of the inverter switch.

VI. Conclusion

In this paper, a control algorithm for seamless transfer of three-phase utility-interactive inverters is proposed. By controlling the capacitor voltage in both grid-connected and stand-alone modes the proposed method is capable of providing critical loads with a stable and seamless voltage during the whole transition period including both clearing time and control-mode-change transition. Some drawbacks of the previous work [7] have been overcome: 1) The proposed method is able to regulate instantaneous values of injected current during the transient. 2) An LCL filter design method based on the exact LCL model is proposed to meet the harmonic limits by considering the ripple rate of the grid current in the grid-side inductance calculation. The proposed control method has been validated through simulation and experiment.

REFERENCES

[1] IEEE Standard for Interconnecting Distributed Resources with Electric Power Systems, IEEE Standard 1547, 2003.

[2] R. Tirumala, N. Mohan, and C. Henze, "Seamless transfer of grid-connected PWM inverters between utility-interactive and stand-alone modes," in *Proc IEEE Appl. Power. Electron. Conf. Expo.*, 2002, pp. 1081–1086.

[3] S. Jung, Y. Bae, S. Choi, and H. Kim, "A low cost utility interactive inverter for residential fuel cell generation," *IEEE Trans. Power Electron.*, vol. 22, no. 6, pp. 2293–2298, Nov. 2007.

[4] G. Q. Shen, D. H. Xu, and X. M. Yuan, "A novel seamless transfer control strategy based on voltage amplitude regulation for utility-interconnected fuel cell inverters with an LCL-filter," in *Proc. IEEE Power Electron. Spec. Conf.*, 2006, pp. 1–6.

[5] T. Hwang, K. Kim, and B. Kwon, "Control strategy of 600 kW E-BOP for molten carbonate fuel cell generation system," in *Proc Int. Conf. Elect. Mach. Syst.*, 2008, pp. 2366–2371.

[6] Z. Yao, L. Xiao, and Y. Yan, "Seamless transfer of single-phase grid-interactive inverters between grid-connected and stand-alone modes," *IEEE Trans. Power Electron.*, vol. 25, no. 6, pp. 1597–1603, Jun. 2010.

[7] H. Kim, T. Yu, and S. Choi, "Indirect current control algorithm for utility interactive inverters in distributed generation systems," *IEEE Trans. Power Electron.*, vol. 23, no. 3, pp. 1342–1347, May 2008.

[8] M. Liserre, F. Blaabjerg, and S. Hansen, "Design and control of an LCL filter based active rectifier," *IEEE Trans. Ind. Appl.*, vol. 38, no. 2, pp. 299–307, Sep./Oct. 2001.

[9] T. C. Y. Wang, Z. Ye, G. Sinha, and X. Yuan, "Output filter design for a grid-interconnected three-phase inverter," in *Proc. Power Electron. Spec. Conf.*, Jun. 2003, vol. 2, pp. 779–784.

[10] N. Mohan, W. P. Robbin, and T. Undeland, *Power Electronics: Converters, Applications, and Design*, 2nd ed. New York: Wiley, 1995.

[11] P. C. Loh, M. J. Newman, D. N. Zmood, and D. G. Holmes, "Improved transient and steady state voltage regulation for single and three phase uninterruptible power supplies," in *Proc. 32nd Ann. IEEE Power Electron. Spec. Conf.*, 2001, pp. 498–503.

[12] F. Blaabjerg, R. Teodorescu, M. Liserre, and A. Timbus, "Overview of control and grid synchronization for distributed power generation systems," *IEEE Trans. Ind. Electron.*, vol. 53, no. 5, pp. 1398–1409, Oct. 2006.

[13] M. Liserre, A. Dell'Aquila, and F. Blaabjerg, "Stability improvements of an LCL-filter based three-phase active rectifier," in *Proc. IEEE Power Electron. Spec. Conf.*, Jun. 2002, vol. 3, pp. 1195–1201.

[14] R. Teodorescu and F. Blaabjerg, "Flexible control of small wind turbines with grid failure detection operating in stand-alone or grid-connected mode," *IEEE Trans. Power Electron.*, vol. 19, no. 5, pp. 1323–1332, Sep. 2004.

[15] N. Pogaku, M. Prodanovic, and T. C. Green, "Modeling, analysis and testing of autonomous operation of an inverter-based microgrid," *IEEE Trans. Power Electron.*, vol. 22, no. 2, pp. 613–625, Mar. 2007.

Junbum Kwon was born in Seoul, Korea, in 1982. He received the B.S. and M.S. degrees from the Department of Control and Instrumentation Engineering from Seoul National University of Science and Technology, Seoul, Korea, in 2007 and 2010, respectively. He is currently an Engineer with the Research and Development Center, LS Industrial Systems, Anyang, Korea. His research interests include three-phase grid connected inverter for renewable energy and insulation coordination design, thyristor valve design for HVDC.

Sunjae Yoon was born in Seoul, Korea, in 1986. She received the B.S. and M.S. degrees from the Department of Control and Instrumentation Engineering from Seoul National University of Science and Technology, Seoul, Korea, in 2009 and 2011, respectively. She is currently an Engineer with the Research and Development Center, LS Industrial Systems, Anyang, Korea. Her research interests include grid-connected inverters for fuel cell and photovoltaic generation systems.

Sewan Choi (S'92–M'96–SM'04) received the B.S. degree in electronic engineering from Inha University, Incheon, Korea, in 1985 and the M.S. and Ph.D. degrees in electrical engineering from Texas A&M University, College Station, TX, in 1992 and 1995, respectively.

From 1985 to 1990, he was with Daewoo Heavy Industries as a Research Engineer. From 1996 to 1997, he was a Principal Research Engineer at Samsung Electro-Mechanics Company, Korea. In 1997, he joined the Department of Control and Instrumentation Engineering, Seoul National University of Science and Technology, Seoul, Korea, where he is currently a Professor. His research interests include power conversion technologies for renewable energy systems and energy storage systems and dc-dc converters and battery chargers for electric vehicles.

Dr. Choi is an Associate Editor of the IEEE TRANSACTIONS ON POWER ELECTRONICS and IEEE TRANSACTIONS ON INDUSTRY APPLICATIONS.